

Supporting information for

Site Dependent Catalytic Water Dissociation on Anisotropic Buckled Black Phosphorous Surface

Adyasa Priyadarsini and Bhabani S. Mallik*

Department of Chemistry, Indian Institute of Technology Hyderabad, Sangareddy 502285, Telangana India

1. Stepwise Collective Variables (CVs)

Our defined collective variables are in the form of a coordination number among the reactive species and reactive sites. For step 1, CV1 and CV2 represent the CN between $P_a(a=ZZ/AC/bulk)-O_a$ and O_a-O_{ext} as depicted in Figure 2(a). For step 2, the CVs (Figure 2(b)) represent the decreasing and increasing CN among O_b-H_a and O_a-H_a , respectively. Figures 2(c) and 2(d) represent the direct and indirect mechanism of step 3. In the direct mechanism, CV1 and CV2 represent the O_a-O_c CN and O_c-O_e CN, here O_e belongs to the spectator water molecule. For the indirect mechanism, the water molecule is the nucleophile and OH^- is the external proton abstractor, following which O_e belongs to the OH^- and O_c belongs to the water molecule. Hence CV1 and CV2 are depicted as CN among O_a-O_c and O_e-H_c respectively.

2. Step 1 [OH^* formation]: Site Dependent Reactivity

We choose 3 different sites for observation, namely zigzag, armchair, and bulk. The closest water molecules properly oriented towards the mentioned sites are selected. A basic medium of 1M allows us to add 1 NaOH to the system, preventing the overpopulation of OH^- and keeping surface oxidation under check. The OH^- acts as the reactive species, prepared by removing one of the protons away from the OH^- and the system neutrality is maintained by adding one Na^+ . Direct adsorption of OH^- leaves us with one probable choice of collective variable, i.e., the coordination number between $P_a(a=ZZ/AC/Bulk)$ and O_a . The second CV is defined considering the non-bonded distance between the oxygen (O_{ext}) of an external water molecule and O_a . No wall potentials are added as the solver properly explores the product state. CV1 and CV2 range between 0 to 1 and 1 to 0, respectively. The external water molecule is kept static at its position so that a fixed cutoff distance can be maintained throughout the metadynamics simulation. The simulations are run for 500 steps, with Gaussian hills worth $0.45 \text{ kcal mol}^{-1}$ being added every 10 NVT steps. The gamma function for well-tempered metadynamics is 15. The OH^* adsorption free energy barriers, obtained by exploring the contour plots from well-tempered metadynamics run, are minimum for ZZ, with a value of $3.69 \text{ kcal mol}^{-1}$, followed by AC and bulk with values 4.11 and $5.09 \text{ kcal mol}^{-1}$. The contour plot along with different reactive states of step 1 are depicted in Figure S1(a-d), (e-h), and (i-l) for ZZ, AC, and bulk sites, respectively.

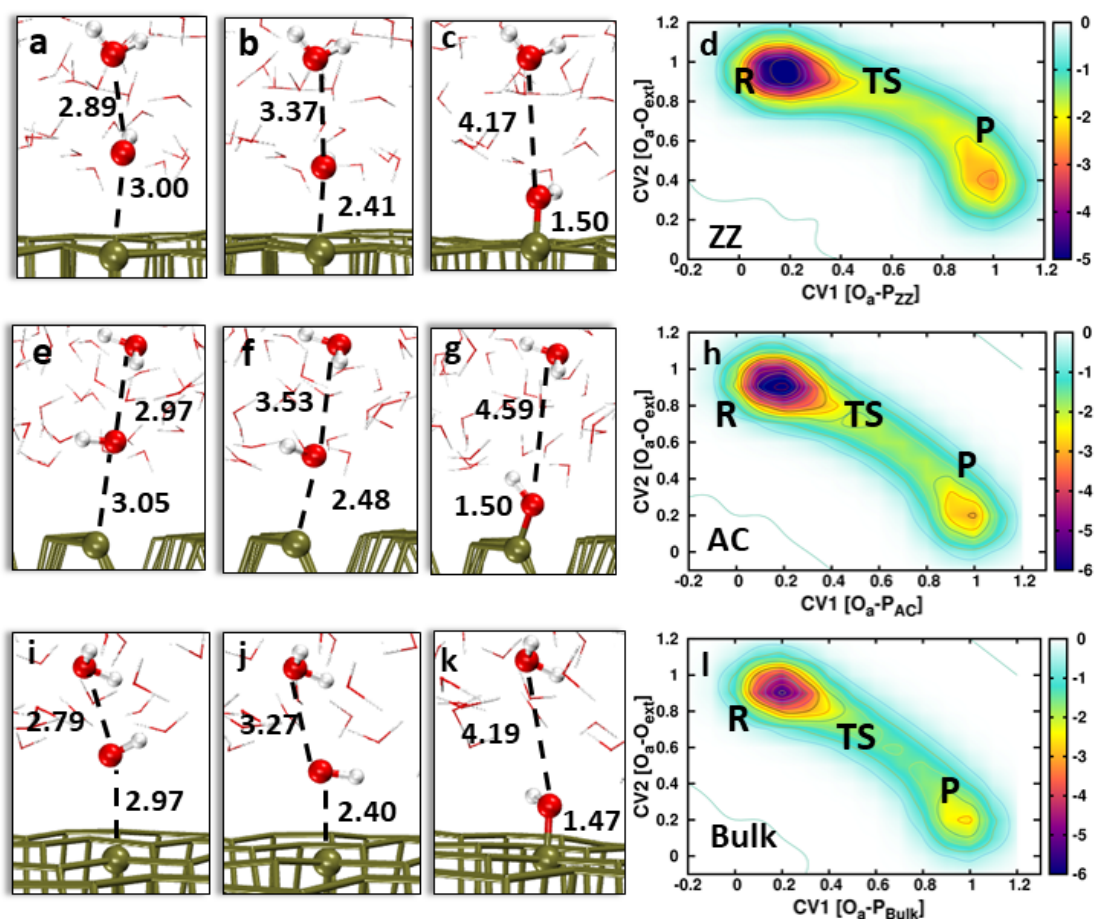


Figure S1. Represents the reactant, transition state, product, and surface contour plot obtained from the metadynamics simulation of the first step of the OER catalyzed by bi-layer BP centered at (a-d) ZZ, (e-h) AC, and (i-l) bulk.

Table S1. The fixed distance cutoff, p , q defined for CV1 and CV2 along with the Gaussian hill parameters, and the free energy barrier obtained for the first step of the OER catalyzed by BP.

| | CV1 | | | CV2 | | | Hill height (kcal mol ⁻¹) | Frequency | γ | Scale | ΔG (kcal mol ⁻¹) |
|-------------|-----|----|----------------|-----|----|----------------|--|-----------|----------|-------|--------------------------------------|
| | P | q | d _o | p | q | d _o | | | | | |
| ZZ | 8 | 18 | 2.5 | 10 | 22 | 4.0 | 0.45 | 10 | 15 | 0.1 | 3.69 |
| AC | 8 | 18 | 2.6 | 10 | 22 | 4.0 | 0.45 | 10 | 15 | 0.1 | 4.11 |
| Bulk | 8 | 18 | 2.6 | 10 | 22 | 3.6 | 0.45 | 10 | 15 | 0.1 | 5.09 |

3. Step 2 [O* formation]: Site Dependent Reactivity

OH* formation is followed by the proton abstraction by the reactive OH⁻ and formation of O*. As a proton transfer step, it is bound to be less energy demanding, already proven by the gas phase calculation of heterogeneous catalyst mediated OER^{1,2}. Our previous studies on undoped and doped graphene-based catalysis study using Langevin metadynamics results in the second and 4th OER step to be the least energy-demanding as they involve simple thermodynamically susceptible proton transfer³. Among the

two CVs defined, CV1 represents the CN between O_b and H_a , taking values within 0 to 1 for non-bonded to the covalently bonded system. CV2 is denoted for O_a and H_a CN and ranges within 1-0. The electronic and physical parameters set for well-tempered metadynamics are provided in Table S2. As expected, the proton transfer barriers for ZZ, AC, and bulk are calculated to be 1.21, 2.16, 1.81 kcal mol⁻¹, quite small-scale as compared to step 1 and step 3. The reactant, transition state, product, and the free energy plot obtained by weighing the two CVs are depicted in Figure S2(a-d), (e-h), and (i-l) for ZZ, AC, and bulk sites, respectively.

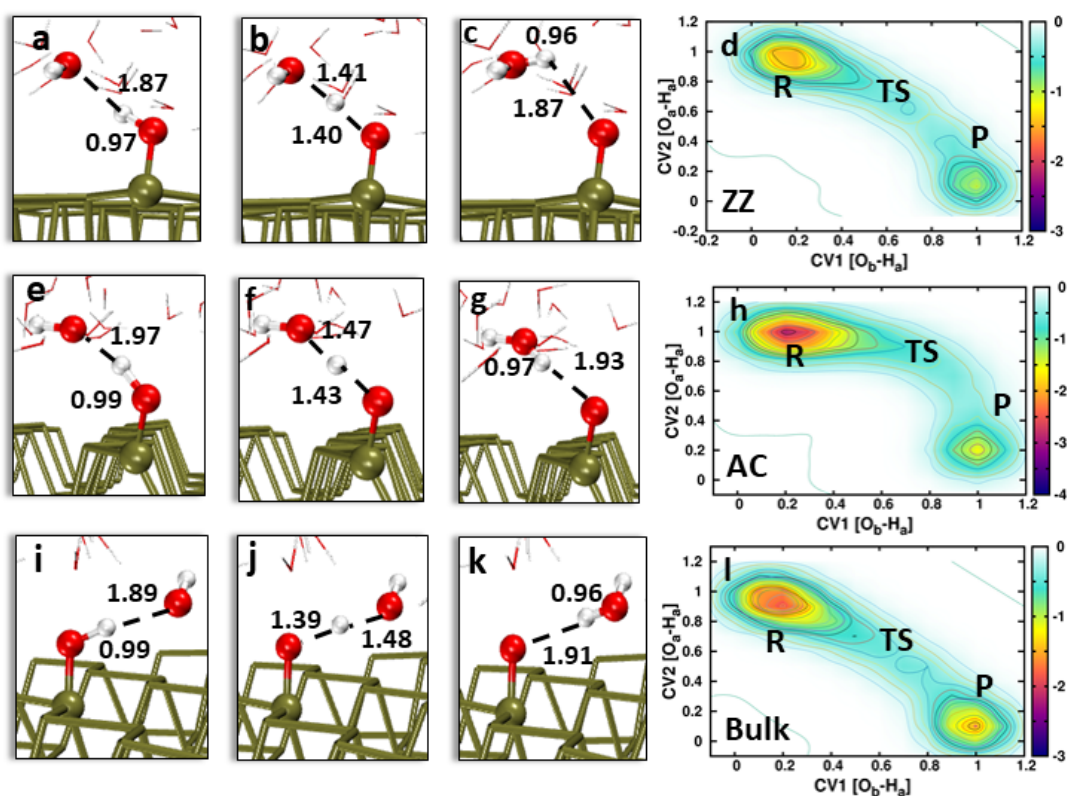


Figure S2. Represents the reactant, transition state, product, and surface contour plot obtained from the metadynamics simulation of the second step of the OER catalyzed by bi-layer BP centered at (a-d) ZZ, (e-h) AC, and (i-l) bulk.

Table S2. The fixed distance cutoff, p , q defined for CV1 and CV2 along with the Gaussian hill parameters, and the free energy barrier obtained for the second step of the OER catalyzed by BP.

| | CV1 | | | CV2 | | | Hill height (kcal mol ⁻¹) | Frequency | γ | Scale | ΔG (kcal mol ⁻¹) |
|-------------|-----|-----|-------|-----|-----|-------|--|-----------|----------|-------|--------------------------------------|
| | p | q | d_o | P | q | d_o | | | | | |
| ZZ | 8 | 18 | 1.6 | 8 | 18 | 1.6 | 0.40 | 5 | 15 | 0.1 | 1.21 |
| AC | 8 | 18 | 1.6 | 8 | 18 | 1.9 | 0.40 | 5 | 15 | 0.1 | 2.16 |
| Bulk | 8 | 18 | 1.5 | 8 | 18 | 1.6 | 0.40 | 5 | 15 | 0.1 | 1.81 |

Table S3. The bonded and non-bonded parameters p, q, and fixed distance cutoff used for two collective variables in two different mechanisms.

| | Mechanism 1 | | | | | | Mechanism 2 | | | | | |
|-------------|---|----|----------------|---|----|----------------|---|----|----------------|---|----|----------------|
| | CV1 CN [O _a -O _c] | | | CV2 CN [O _a -O _e] | | | CV1 CN [O _a -O _c] | | | CV2 CN [H _c -O _e] | | |
| | p | q | d _o | p | q | d _o | p | q | d _o | P | Q | d _o |
| ZZ | 8 | 18 | 2.2 | 10 | 22 | 4.0 | 8 | 18 | 2.2 | 8 | 18 | 2.1 |
| AC | 8 | 18 | 2.3 | 10 | 22 | 4.2 | 8 | 18 | 2.2 | 8 | 18 | 2.0 |
| Bulk | 8 | 18 | 2.3 | 10 | 22 | 4.1 | 8 | 18 | 2.2 | 8 | 18 | 1.9 |

Table S4. Different Gaussian hill parameters and free energy barriers along with standard deviation obtained from 3 different runs for the third step of OER at the zigzag, armchair, and bulk site. All the parameters are tabulated for mechanisms 1 and 2.

| Mechanism 1 | | Hill height (kcal mol ⁻¹) | Frequency | K (kcal mol ⁻¹) [CV1] [CV2] | | γ | Scale | ΔG (kcal mol ⁻¹) | $\bar{x} \pm \sigma$ | | |
|-------------|-------|--|-----------|--|------|----|-------|----------------------------------|----------------------|----------------------------------|----------------------|
| ZZ | Set 1 | 1.25 | 5 | 4.0 | - | 15 | 0.1 | 7.18 | 7.59±0.33 | | |
| | Set 2 | 1.75 | 7 | 4.0 | - | 15 | 0.1 | 7.60 | | | |
| | Set 3 | 2.25 | 9 | 4.0 | - | 15 | 0.1 | 7.99 | | | |
| AC | Set 1 | 1.25 | 5 | 4.0 | - | 20 | 0.1 | 9.04 | 9.04±0.01 | | |
| | Set 2 | 1.75 | 7 | 4.0 | - | 20 | 0.1 | 9.02 | | | |
| | Set 3 | 2.25 | 9 | 4.0 | - | 20 | 0.1 | 9.06 | | | |
| Bulk | Set 1 | 1.25 | 5 | 8.0 | - | 20 | 0.1 | 12.81 | 12.80±0.09 | | |
| | Set 2 | 1.75 | 7 | 8.0 | - | 20 | 0.1 | 12.68 | | | |
| | Set 3 | 2.25 | 9 | 8.0 | - | 20 | 0.1 | 12.91 | | | |
| Mechanism 2 | | Hill height (kcal mol ⁻¹) | Frequency | K (kcal mol ⁻¹) [CV1] [CV2] | | γ | Scale | ΔG1 (kcal mol ⁻¹) | $\bar{x} \pm \sigma$ | ΔG2 (kcal mol ⁻¹) | $\bar{x} \pm \sigma$ |
| ZZ | Set 1 | 1.25 | 5 | 4.0 | 4.0 | 15 | 0.1 | 1.24 | 1.81 | 6.24 | 5.74 |
| | Set 2 | 1.75 | 7 | 5.0 | 5.0 | 15 | 0.1 | 1.89 | ±0.44 | 5.73 | ±0.49 |
| | Set 3 | 2.25 | 9 | 5.0 | 6.0 | 15 | 0.1 | 2.31 | | 5.25 | |
| AC | Set 1 | 1.25 | 5 | 14.0 | 10.0 | 25 | 0.1 | 5.11 | 4.87 | 4.26 | 4.28 |
| | Set 2 | 1.75 | 7 | 16.0 | 11.0 | 25 | 0.1 | 4.88 | ±0.24 | 4.23 | ±0.08 |
| | Set 3 | 2.25 | 9 | 16.0 | 12.0 | 25 | 0.1 | 4.62 | | 4.36 | |
| Bulk | Set 1 | 1.50 | 5 | 16.0 | 10.0 | 25 | 0.1 | 3.26 | 3.38 | 8.50 | 8.25 |
| | Set 2 | 2.00 | 7 | 18.0 | 11.0 | 25 | 0.1 | 3.49 | ±0.11 | 8.12 | ±0.22 |
| | Set 3 | 2.50 | 9 | 18.0 | 11.0 | 25 | 0.1 | 3.39 | | 8.13 | |

4. Free Energy Plot of third Step [OOH* formation]

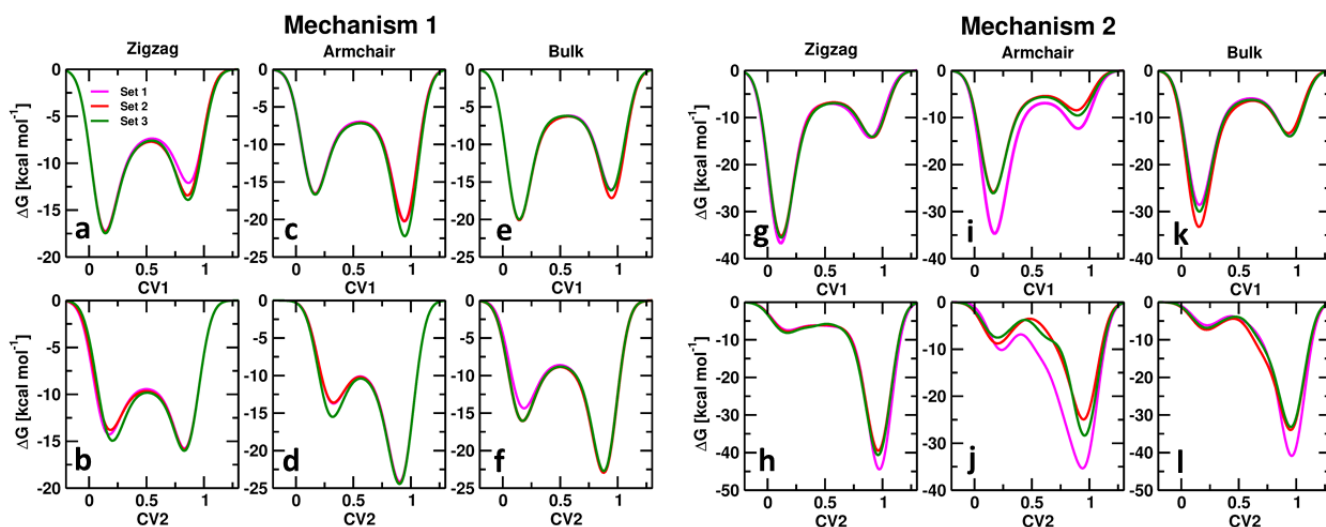


Figure S3. Represent the 1D plot of free energy barrier in terms of individual CVs as obtained from the metadynamics simulation of step 3 of OER following (a-f) mechanism 1 and (g-l) mechanism 2 taking place at ZZ, AC, and bulk site.

5. Rate Constant

The elementary steps of the OER reactions follow first-order reaction kinetic. The rate of reaction of an elementary reaction is given as⁴,

$$k = A e^{\frac{E_a}{k_b T}} = \frac{k_b t Q^{TS}}{h Q} e^{\frac{E_a}{k_b T}}$$

where k = the rate constant in s^{-1} , k_b = Boltzmann constant in $eV K^{-1}$, T = reaction temperature in K, E_a = is the activation barrier in eV. The partition functions of the transition states and the ground states are given as Q_{TS} and Q . In the rate equation $\frac{k_b t Q^{TS}}{h Q}$ is the prefactor A, chosen to be $10^{-3} s^{-1}$ for all elementary reactions⁴. We can directly use the rate equation to calculate the rate constant for the rate determining step of OER. The rate constants for the 3rd step of OER, catalyzed by BP at the ZZ site, are calculated for mechanism 1 and 2. The rate constant for the formation of the hydroperoxo species through mechanism 1 and mechanism 2 is $2956.92 \times 10^4 s^{-1}$, $2811.90 \times 10^4 s^{-1}$, respectively.

Table S4. Comparative table for the activation energy of the rate determining step of OER, obtained from metadynamics simulation, catalyzed by undoped graphene⁵, doped graphene³, and BP.

| | Involved Mechanism | ΔG [kcal mol ⁻¹] |
|------------------|--------------------|--------------------------------------|
| Undoped graphene | Mechanism 1 | 21.19±0.51 |
| N-doped graphene | Mechanism 1 | 18.23 ±0.48 |
| P-doped graphene | Mechanism 1 | 17.88 ±0.76 |
| B-doped graphene | Mechanism 1 | 15.97 ±0.51 |
| S-doped graphene | Mechanism 1 | 14.73 ±0.92 |
| BP | Mechanism 1 | 7.59 ±0.33 |
| | Mechanism 2 | 7.62±0.11 |

REFERENCES

- (1) Fortunelli, A.; Iii, W. A. G.; Sementa, L.; Barcaro, G. Optimizing the Oxygen Evolution Reaction for Electrochemical Water Oxidation by Tuning Solvent Properties. *Nanoscale* **2015**, *7*, 4514–4521.
- (2) Lucking, M.; Sun, Y.-Y.; West, D.; Zhang, S. A Nucleus-Coupled Electron Transfer Mechanism for TiO₂-Catalyzed Water Splitting. *Phys. Chem. Chem. Phys.* **2015**, *17*, 16779–16783.
- (3) Priyadarsini, A.; Mallik, B. S. Effects of Doped N, B, P, and S Atoms on Graphene toward Oxygen Evolution Reactions. *ACS Omega* **2021**, *6*, 5368–5378.
- (4) Guo, W.; Lian, X. Kinetics Mechanism Insights into the Oxygen Evolution Reaction on the (110) and (022) Crystal Facets of β -Cu₂V₂O₇. *Catal. Sci. Technol.* **2020**, *10*, 5129–5135.
- (5) Priyadarsini, A.; Mallik, B. S. Comparative First Principles-Based Molecular Dynamics Study of Catalytic Mechanism and Reaction Energetics of Water Oxidation Reaction on 2D-Surface. *J Comput Chem* **2021**, *42*, 1138–1149.